Iceland Liechtenstein Norway grants
"Working together for a green, competitive and inclusive Europe"

GREENCAM for tomorrow

UNIVERSITY OF BUCHAREST
VIRTUTE ET SAPIENTIA

NTNU
Norwegian University of Science and Technology

UNIVERSITATEA DIN BUCUREȘTI
VIRTUTE ET SAPIENTIA

FACULTY OF CHEMISTRY

DEPARTMENT OF ORGANIC CHEMISTRY, BIOCHEMISTRY AND CATALYSIS

MSc Thesis – Report 3

Catalytic amino acid production from biomass-derived intermediates

MASTER: CHEMISTRY OF ADVANCED MATERIALS

STUDENT: MARA ALEXANDRA BADEA

SCIENTIFIC COORDINATOR: Prof. Dr. Simona-Margareta Coman

February 22, 2022

Disclaimer: This was realised with the EEA Financial Mechanism 2014-2021 financial support. Its content (text, photos, videos) does not reflect the official opinion of the Programme Operator, the National Contact Point and the Financial Mechanism Office. Responsibility for the information and views expressed therein lies entirely with the author(s).

CONTENT

Introduction

Amino acids are valuable products for industry due to their versatility. Nowadays, glutamic acid, lysine, methionine and threonine cover more than 95% of the total market volume [1]. This is why the researchers focus now in developing on two directions: the discovery of new production methods regarding this four amino acids and the discovery of production methods regarding the rest of amino acids. Today, amino acids are primarily manufactured via microbial cultivation processes, which are costly, are time consuming, and require extensive separations processes. The development of efficient chemical methods to convert abundant and renewable feedstocks into amino acids is, therefore, highly attractive but it have been largely unsuccessful to date. As an alternative, chemocatalytic approaches to produce amino acids from renewable feedstocks such as bio-based sugars could offer a rapid and potentially more efficient means of amino acid synthesis, but efforts to date have been limited by the development of facile chemistry and associated catalyst materials to selectively produce α-amino acids.

In our knowledge, only one recent report on a heterogeneous catalyst that directly transforms lignocellulosic biomass-derived α-hydroxyl acids into α-amino acids, including alanine, leucine, valine, aspartic acid, and phenylalanine in high yields exist in literature [2]. In this work the authors showed ruthenium nanoparticles supported on carbon nanotubes (Ru/CNT) exhibit exceptional efficiency compared with catalysts based on other metals, due to the unique, reversible enhancement effect of NH_3 on Ru in dehydrogenation.

The CNT application in heterogeneous catalysis is based on their specific important characteristics such as: (i) resistance to acid/basic media, (ii) possibility to control, up to certain limits, the porosity and surface chemistry and (iii) easy recovery of precious metals by support burning resulting in a low environmental impact [3]. The combination of these properties makes CNT attractive and competitive catalyst supports by comparison with activated carbons.

Like for classical carbon materials used in catalysis the possibility of chemical or thermal activation, in order to modify the nature and concentration of surface functional groups, has been studied in the case of CNT. Among the different techniques that have been applied for the more or less pronounced surface oxidation, nitric acid treatments are the most common and it has been shown that surface oxygen functionalities like carboxylic groups can be introduced on the outer and possibly inner walls of the CNT [4]. In the case of MWCNT the main significant structural modification occurs on the nanotubes tip and can result(s) in their opening, and the formation of edges and steps on the graphene sheets is possible [5].

Deposition of different metals (i.e., silver, cobalt, cerium) on nitric-acid treated MWCNT showed the critical factor to well dispersed nanoparticles is the oxidation step [3].

Objectives

The aim of this work was to develop efficient heterogeneous catalysts able to directly transform lignocellulosic biomass-derived lactic acid into alanine. For this a series of Ru-based heterogeneous catalysts with oxidised MWCNT were prepared and characterised.

Different oxidation processes were applied in the view of producing functionalized CNTs and their use as carrier for ruthenium deposition, in the next step of the research. By using such type of carriers (i.e., as-received CNT and oxidized CNT) Ru-based catalysts with different catalytic features related to the metal dispersion, location (ruthenium in- and out-tubes) and reduction degree, can be easily created.

Experimental part

All the chemicals and reagents were of analytical purity grade, purchased from Sigma-Aldrich and used without further purification. All the chemicals and reagents were of analytical purity grade, purchased from Sigma-Aldrich and used without further purification. Two kind of multi-walled carbon nanotubes (MWCNTs) were purchased from Sigma-Aldrich with the following features: (1) preparation method Catalytic Chemical Vapor Deposition (CVD) (CoMoCAT®), over 95% carbon, O.D×L/6-9 nm × 5 μm and armchair configuration, and (2) preparation method Catalytic Chemical Vapor Deposition, over 90% carbon basis, D×L/110-170 nm × 5-9 μm and armchair configuration. Hydrated ruthenium chloride ($RuCl_3xH_2O$) had ~37% Ru basis. PTFE membrane filters with 0.45 μm pore size were purchased from Merck.

a) Materials preparation methodology

The oxidation of MWCNTs has as result the opening up of carbon nanotubes, their purification and functionalization. Eight different oxidation procedures were performed in order to establish the optimum oxidation conditions in the view of the synthesis of an optimal functionalized CNTs structure. The prepared samples and the oxidation conditions are summarized in Table 1. For the first seven procedures CoMoCAT® MWCNT were used to produce the CNT_{ox}-1 - CNT_{ox}-7 samples while the CNT_{ox}-8 sample was produced from

MWCNTs with 95% carbon, O.D×L/6-9 nm × 5 μm and armchair configuration. In order to minimize tube damage, a low power sonicating bath and a relatively low acid exposure time were used. The oxidation processes were carried out either under reflux, by using a sonication bath or by refluxing followed by sonication. Nitric acid (65 wt%) or a mixture of HNO_3 and H_2SO_4 were used as oxidation reagents and the oxidation time was varied from 1h to 3h. Irrespective of the applied methodology the resulted solid was washed up to neutral pH and dried at 80°C for 24 h. All procedures methodologies are detailed in Annex 1.

Table 1. The oxidation conditions used for the synthesis of CNT_{ox} samples

Entry	Sample	m_{MWCNT} (g)	V_{HNO3} (mL)	V_{H2SO4} (mL)	V_{H2O2} (mL)	Procedure		
						Ultrasonication time (h)	Reflux	
							Time (h)	Temperature (°C)
1	CNT_{ox}-1	2	200	-	-	3	-	-
2	CNT_{ox}-2	1	200	-	-	3	2	80 (1h) 100 (1h)
3	CNT_{ox}-3	1	200	-	-	3	2	80
4[a]	CNT_{ox}-4	0.3	14	42	-	2	15 min	60
5[b]	CNT_{ox}-5	0.3	14	42	7.5	2	15 min	60
6	CNT_{ox}-6	0.1	7.5	-	7.5	3	15 min	60
7	CNT_{ox}-7	0.1	-	-	12.5	-	72	65
8[c]	CNT_{ox}-8	0.1	10	-	-	3	24	r.t.

[a] - 70 mL mixture of HNO_3 (65wt%) and H_2SO_4 (8M), mechanical stirring; [b] - 70 mL mixture of HNO_3 (65wt%) and H_2SO_4 (3M), mechanical stirring; [c]- distillation of CH_2Cl_2

b) Characterization techniques

Prepared samples were characterized by adsorption-desorption isotherms of liquid nitrogen at -196 °C, X-ray diffraction (XRD), temperature programmed desorption of H_2 and NH_3 (H_2-TPD and NH_3-TPD), IR diffuse reflectance with Fourier transform (DRIFT) and Raman spectroscopy, and thermogravimetric-differential thermal analysis (TG-DTA).

Textural characteristics (surface area, pore volume and pore diameter) were determined from the adsorption-desorption isotherms of nitrogen at -196 °C using a Micromeritics ASAP 2020 Surface Area and Porosity Analyzer.

Powder X-ray Diffraction patterns were collected at room temperature using a Shimadzu XRD-7000 apparatus with the Cu Kα monochromatic radiation of 1.5406 Å, 40 kV, 40 mA at a scanning rate of 1.0 2θ min^{-1}, in the 2θ range of 10º–90º.

Hydrogen chemisorption and NH_3-temperature programmed desorption (NH_3-TPD) were recorded using a Micromeritics apparatus – Autochem II (Chemisorption Analyzer). Approximately 20 mg freshly reduced Ru/CNT was heated at 650°C unde N_2 for 0.5 h to remove the hydrogen adsorbed on Ru atoms. After that, the temperature was reduced to 150°C and waited until baseline became stable. Subsequently, successive doses of H_2 gas were provided. The measurements for NH_3-TPD were performed in the same manner.

DRIFT spectra were recorded with a Thermo 4700 spectrometer (400 scans with a resolution of 4 cm^{-1}) in the range of 400–4000 cm^{-1}.

Raman spectra were recorded using a microscope equipped triple monochromator. The spectra were acquired in the back-scattering geometry, while for excitation the 514.4 nm line of an Ar^+ laser was focused on the sample by means of an 50 objective, measured directly.

TG-DTA analyses were recorded using a Shimadzu apparatus in a Pt crucible. The heating rate was of 10°C min^{-1}, respectively, starting from room temperature till 850 °C under a nitrogen flow of 50 mL min^{-1}.

Results and discussions

Oxidation of CNTs: Opening up of carbon nanotubes, purification and functionalisation

As the nitrogen adsorption-desorption isotherms of the Ru/CNT samples showed in previous work, the capillarity mainly occurs in the small cylindrical mesopores (inner cavities) and the aggregated pores of CNT, the latter being associated with the larger portion of the total nitrogen adsorption amount. The small fraction of the total nitrogen adsorption amount in the inner cavities indicate that not all ends of nanotubes are opened [6]. However, to improve the adsorption and capillarity of CNTs both the opening-up of the nanotubes and the control of their aggregated pore texture is important.

The simplest method to open nanotubes is their oxidative treatment. It is well known that graphite oxidizes primarily at defects of the hexagonal lattice to create etch pits. When such defect sites are present in the wall of the nanotubes, they become the center of preferential etching. However, nanotubes have additional structural features such as high curvature and helicity, and may contain five- and seven-membered rings, which modify the initiation and also the propagation of oxidation. Particularly for multiwall CNTs, the oxidation tends to start near the tips, providing a mechanism for opening the tubes.

Oxidative treatment of nanotubes results not only in nanotubes open at their tips, but also nanotubes that are thinner in diameter [7]. The concentric layers of multiwall CNTs do not react at the same rate, since each shell has its own tip. It follows that the inner shells might persist longer than the outer ones. Therefore, different oxidation rates are assumed for oxidation of an open multiwall CNTs. The extent of the thinning depends on the duration of treatment.

A further consequence of oxidative treatment is partial functionalization of the tubes; i. e., the nanotubes become covered with carboxyl or hydroxyl groups at their ends. These functional groups make the NTs partially soluble. The number or concentration of the inserted carboxyl groups can be estimated by acid–base titration or NH_3-TPD. The concentration of the surface acid groups on nanotubes opened by various oxidants is in the range of 2×10^{20}–10×10^{20} sites per gram of nanotube [8].

CNT_{ox} samples characterization

XRD

XRD is a valuable tool to probe the internal arrangement of the atomic planes in a chemical substance. In case of carbon nanotubes, after some authors, however, resolution of the diffraction pattern is a complex matter because of the extremely large variation in their size, curvature and the disorder in the packing of the graphene sheets. [9] All these factors combined together affect the reflectance, as well as diffraction line positions and widths from one sample to another.

The X-ray pattern for the pristine CNTs (Figure 1, inset) a sharp well defined diffraction line at 2θ = 25.8° and one smaller line at 43°, corresponding with (002) and (101) planes. According to literature [9] the diffraction line from 25.8° correspond to the spacing between graphene sheets. Besides these out-of-plane ordering reflectances, CNTs also show two lines at 2θ values of 28° and 52° respectively, corresponding with (100) and (102) planes. However, in this case, the XRD pattern does not present the out-of-plane reflectance and in-plane reflectance, thus implying the lack of in-plane ordering in these specific directions.

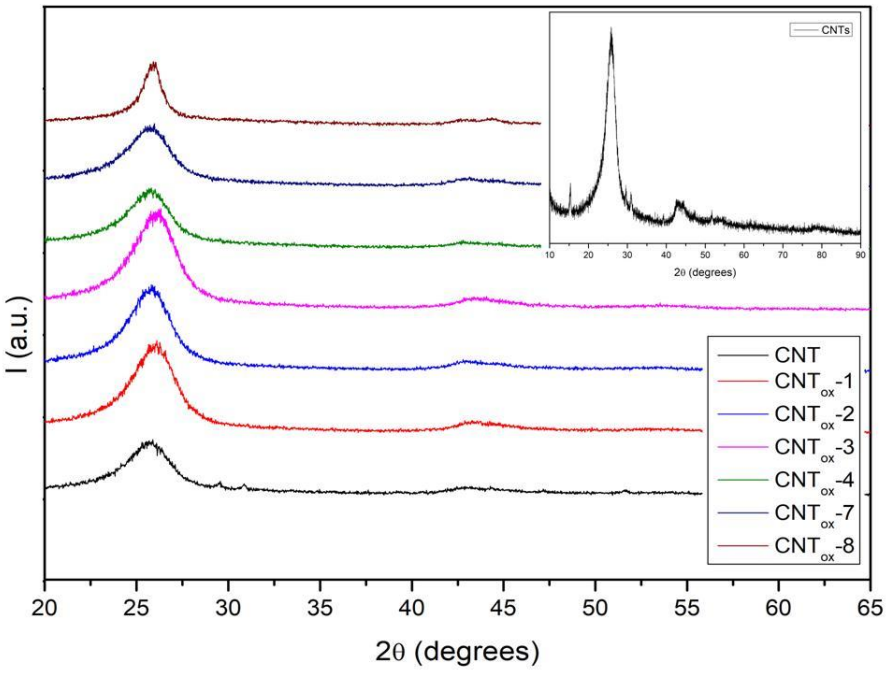

Figure 1. XRD pattern of as-received MWCNTs and oxidised CNTs

Subsequent to acid treatment, the XRD spectra shows a change in the magnitude and the 2θ shifting position of the reflectance lines (Figure 1).

In the case of CNT_{ox}-1, CNT_{ox}-2 and CNT_{ox}-3 samples the intensity of the line at 2θ = 25.8° is higher than that of the pristine CNT, this increases being attributed to a increase in the number of walls of the CNTs. [34] In the case of CNT_{ox}-4, CNT_{ox}-7 and CNT_{ox}-8 the intensity of the line at 2θ = 25.8° is lower than that of the pristine CNT, being attributed to a decrease in the number of walls of the CNTs. The lower intensity has also been related to a lower packing density or the presence of defects. Not less important, the decrease in the intensity of the (002) plane (2θ = 25.8°) is also attributed to the disordered structure of the nanotubes. This disorder is the effect of the attachment of functional groups at the surface and ends of the nanotubes, thus causing steric hinderance and impelling the individual nanotubes to misalign. The comparatively greater height of the (002) plane (2θ = 25.8°) in case of as-received CNTs has also been explained in terms of the greater graphitic character of the tubes.[9] This may only be true if there is a large number of equidistant tubes in the multi-walled CNT so that their reflectances overlap to five a high intensity line.

The shifting of the (002) plane (2θ = 25.8°) toward higher values of 2θ angle from as-received CNTs until CNT_{ox}-8 is a result of an decrease in the intertubular spacing, which in turn indicates a loss in the ordered structure of the nanotubes.

The X-ray diffraction patterns of oxidized CNTs show a relatively greater broadness of the line at 43.3° indicating a lower crystallinity and a greater curvature in the nanotubes surface. According to literature [10], the greater the diameter of CNTs the smaller is its curvature, thus resulting in a larger value of the d-spacing which, in this case, implies a smaller diameter of the tubes.

The broader distribution of peaks in CNT_{ox}-5 and CNT_{ox}-6 as compared to the as-received CNTs reflects the turbostratic character of the nanotubes (Figure 2). This is because the debundling of CNTs decreases the crystalline domains size, resulting in the increased amorphous character of the nanotubes. It has also been reported that a broader distribution of d-spacing results in broader peaks [11] which is also a direct consequence of over-oxidation and loss of graphitic character.

.

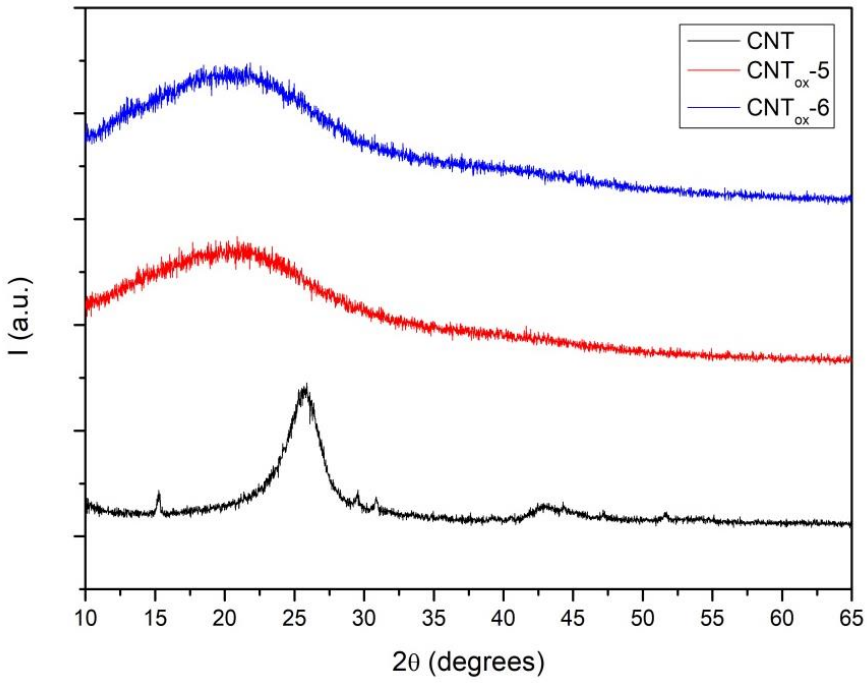

Figure 2. XRD patterns of oxidized (5-6) MWCNTs and as-received MWCNTs for comparison

NH_3-TPD

It is known that the amount and type of oxygen-containing functional groups strongly depends on the treatment methods and their process parameters. In case of nitric acid, the nitronium ion NO_2^+ is believed to be able to attack the aromatic compounds, which is assumed to be the first step in the generation of oxygen-containing functional groups, followed by the formation of carbonyls and their conversion into carboxylic groups and carboxylic anhydrides [12]. In addition, nitrogen-containing groups can also be created by the nitric acid treatment.

Figure 3 shows the NH_3-TPD profiles for the CNT_{ox} samples obtained by HNO_3-treated nanotubes in different conditions (for oxidation conditions see Table 1).

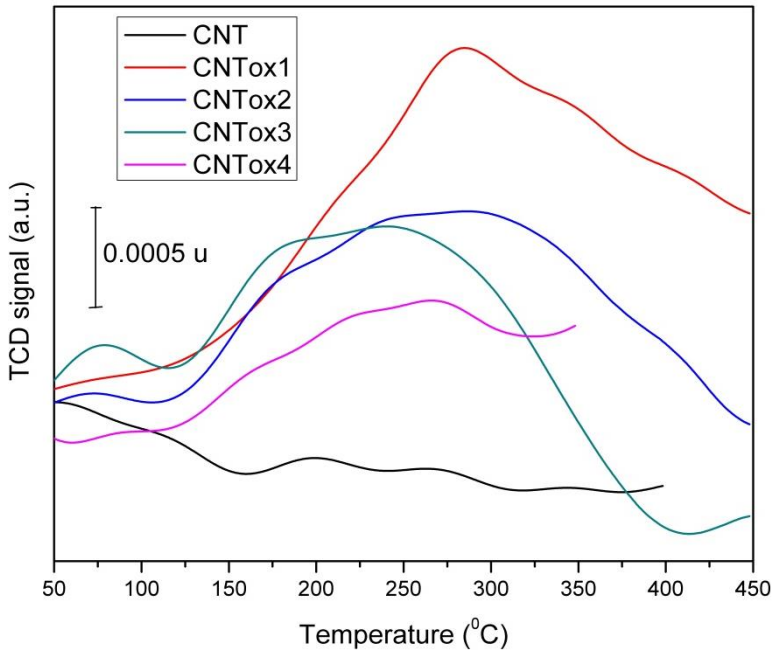

Figure 3. The NH3-TPD profiles of the CNT_{ox} samples

The main ammonia TPD peak appeared at about 260-280 °C (Figure 3), indicating that most of the ammonia molecules are chemisorbed with a medium strength. The shoulder at high temperatures (cca 400°C, CNT_{ox}-1 and CNT_{ox}-2 samples) can be assigned to carboxylic structures, onto which ammonia chemisorbs strongly presumably *via* the formation of ammonium carboxylates. Most of the acidic groups act as primary adsorption centers, which bind additional ammonia molecules weakly through hydrogen bonds [13].

The total desorbed ammonia (mmol/g) varied in order: 0.073 (CNT_{ox}-2) > 0.053 (CNT_{ox}-1) ≥0.052 (CNT_{ox}-3) >> 0.004 (CNT_{ox}-4), which strongly depends on the oxidation procedure conditions.

IR spectroscopy

In Figure 4, IR spectra of the CNTs before and after the oxidation process (CNT_{ox}-1 - CNT_{ox}-4) are presented.

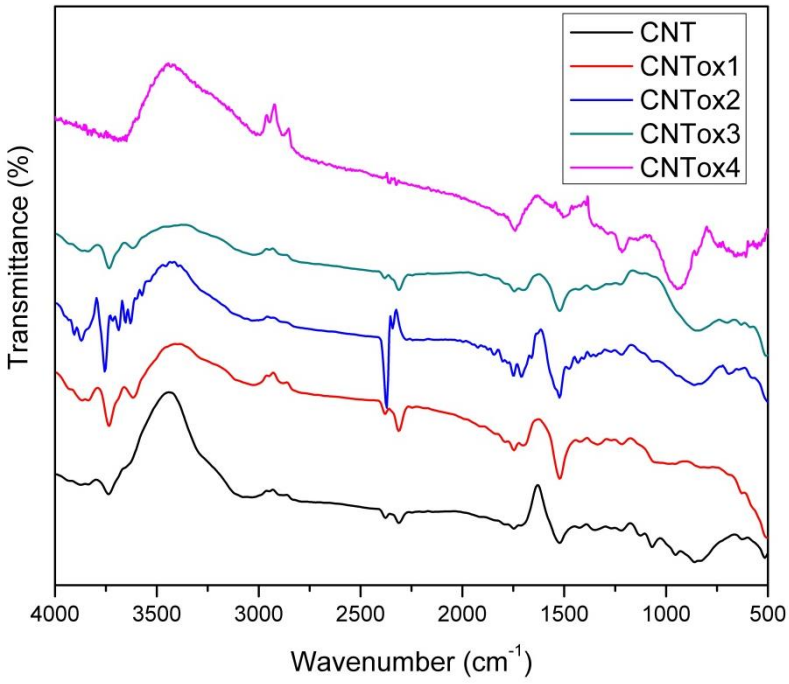

Figure 4. IR spectra of CNT and oxidised CNTs samples (see procedures 1-4 from Annex 1)

The presence of typical C=O and O-H bonds are due to the formation of COOH groups on the nanotubes after acid treatment. This is evident in the IR spectrum shown in Figure 11. Different peaks at 3600-3900 cm^{-1} are assigned to the O-H stretches of terminal carboxyl groups, the peaks at 2800-2944 cm^{-1} can be assigned to the C-H stretch, and the peaks near 1742 cm^{-1} correspond to the carboxylic C=O stretching vibrations. The peak at 1527 cm^{-1} is attributed to the -C=C- stretching mode of the CNTs [14]. IR spectra also indicates the presence of the carbonyl (C=O) (1223 cm^{-1}) groups and the presence of the epoxide groups indicated by the presence of an absorption band in the 910-920 cm^{-1} range, related to the contraction of the C-C bond and the stretching of C-O bonds of the epoxy ring [15].

The highest amounts of -COOH and carbonyl groups were generated on CNT_{ox}5-7 (Figure 5). Unfortunately, a too advanced oxidation lead to a structure collapse as XRD analysis show for the CNT_{ox}-5 and CNT_{ox}-6 samples. Indeed, the IR spectra also shows a high increases of the bands intensity corresponding to the C-H stretch (2800-2944 cm^{-1}) and of those corresponding to the contraction of the C-C bond (910-920 cm^{-1} range) in the detriment of the -C=C- stretching mode (1527 cm^{-1}).

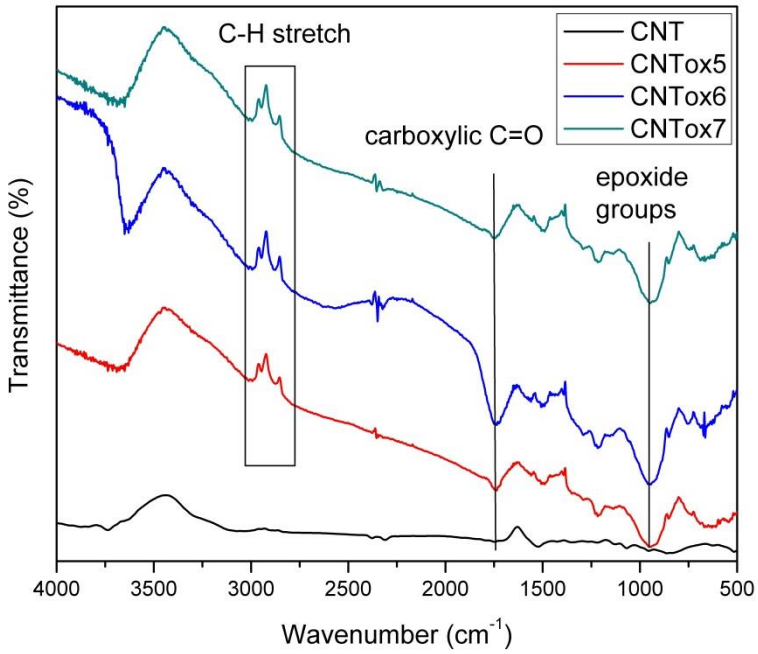

Figure 5. IR spectra of CNT and oxidised CNTs samples
(see procedures 5-7 from Annex 1).

Raman spectroscopy

Raman spectroscopy is a very valuable tool for the characterization of carbon-based nanostructures. The Raman spectrum of as-received CNTs is shown in Figure 6.

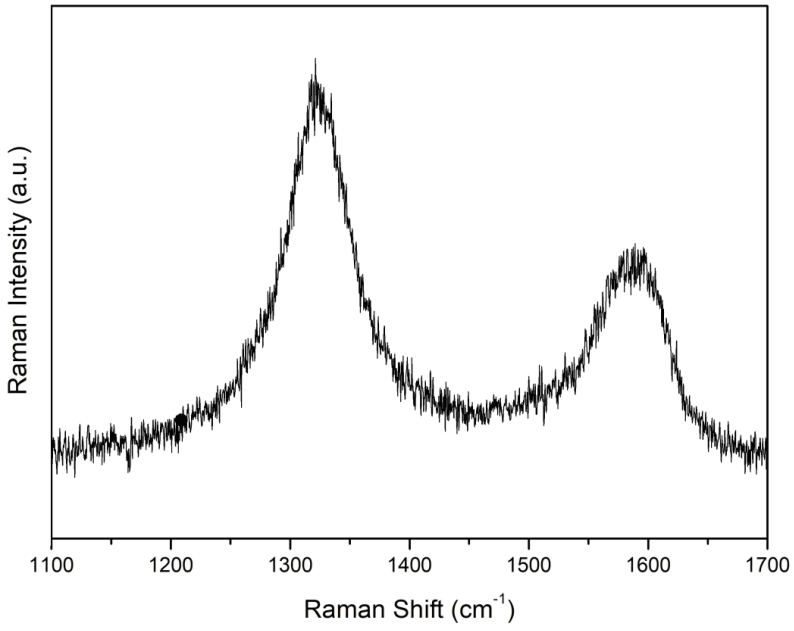

Figure 6. Raman spectra for as-received MWCNTs (i.e., CNT sample)

The Raman spectrum consists of three characteristic bands: D band, G band and D' band. In the as-received carbon nanotubes the D band appears at 1322 cm^{-1}, the G band appears at 1587 cm^{-1} and the D' band appears at 1606 cm^{-1}. The D-band is a disordered induced feature, arising from double resonance Raman scattering process from a non-zero centre phonon mode.[16] The D band is usually attributed to the presence of amorphous or disordered carbon in the CNT samples. The carbon structural disorder is due to the finite or nanosized graphitic planes and other forms of carbon such as rings along with defects on the nanotube walls. The G band originates from in-plane tangential stretching of the carbon-carbon bonds in graphene sheets.[16] The D' band, which appears as a weak shoulder in the G band at higher frequencies, is also a double resonance feature induced by disorder and defects. Also, it should be underlined that the radial breathing modes are too weak to be observed due to the large diameters of the tubes.

The Raman spectra obtained for some of oxidised CNT samples are shown in Figure 7. A slightly up-shift for the G band, indicating an increases of the number of sp^2 carbons, is observed from CNT_{ox}-1 toward the CNT_{ox}-7 sample. This effect usually indicates the strength of the oxidation process: the greater the displacement the stronger the oxidative process. Therefore, CNT_{ox}-7 sample is stronger oxidised than the CNT_{ox}-1 sample. This statement is in agree with the results obtained from DRIFT measurements (Figures 4-5).

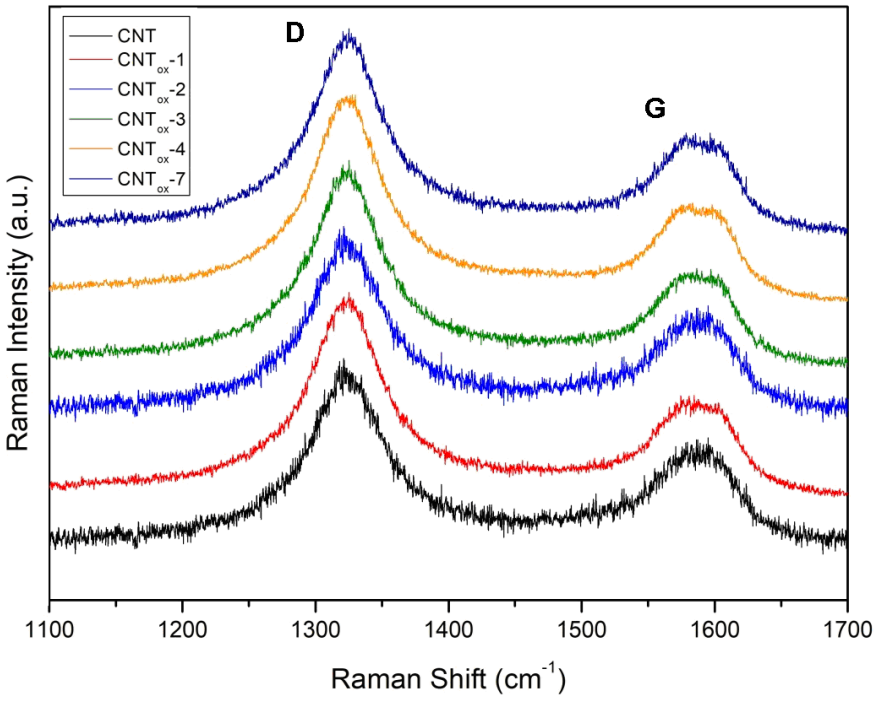

Figure 7. Raman spectra for as-received and oxidized MWCNTs from 1-4 and 7

The Raman spectra of the CNT_{ox}-5, CNT_{ox}-6 and CNT_{ox}-8 samples are presented in Figures 8 and 9. As Raman spectra of CNT_{ox}-5 and CNT_{ox}-6 samples (Figure 8) shows an up-shift of the D band and a slightly decrease in intensity for D and G bands takes place, most probably due to an over oxidation of the CNTs according to Chernyak S.A. and al. [17] This over oxidation also lead to an increased amorphous character of the nanotubes, as corresponding XRD patterns showed (Figure 1).

In the Raman spectrum for CNT_{ox}-8 (Figure 9) a decrease in the wavenumber of the G band accompanied by an increase in the wavenumber of the D band is visible. Moreover, the D' band, corresponding to the defects in the CNT structure is more visible. These new features of the Raman spectra suggest a successful synthesis of an oxidized CNT with a concomitant increase in the number of defects compared to pristine CNT.

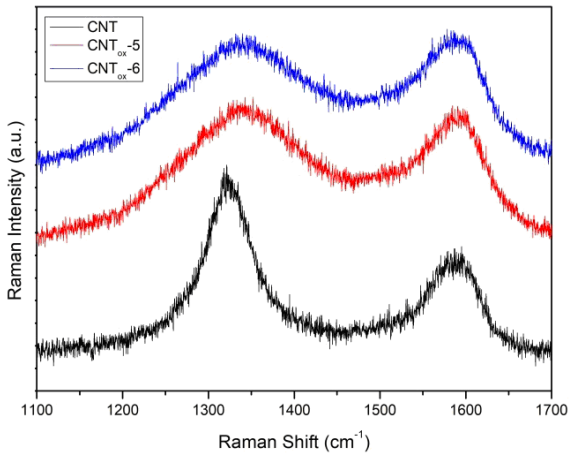

Figure 8. Raman spectra for as-received CNT and CNT_{ox}-5 and CNT_{ox}-6 samples

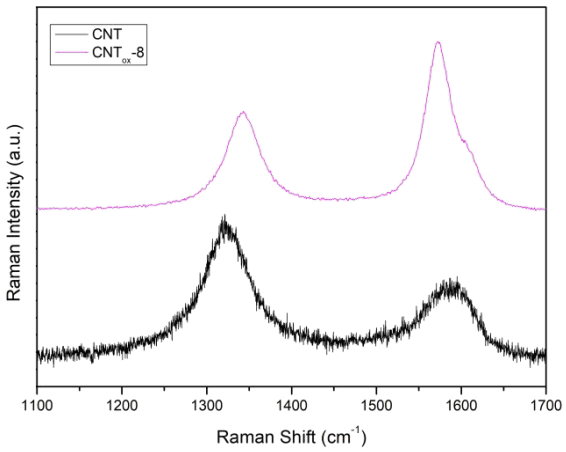

Figure 9. Raman spectra for as-received CNT and CNT_{ox}-8 sample

The intensity ratio of G to D band in the Raman spectra of oxidized samples is presented in the Table 2.

Table 2. I_G/I_D intensity ratios for the treated CNTs

Sample	**Pristine**	**CNT_{ox}-1**	**CNT_{ox}-2**	**CNT_{ox}-3**	**CNT_{ox}-4**	**CNT_{ox}-5**	**CNT_{ox}-6**	**CNT_{ox}-7**	**CNT_{ox}-8**
I_G/I_D	0.63	0.38	0.21	0.37	0.43	0.96	1.01	0.34	1.66

As Table 2 shows the intensity ratio G to D band (I_G/I_D) is almost the same indicating a similar defect population for the CNT_{ox}-1, CNT_{ox}-3 and CNT_{ox}-7 samples. However, compared to the as-received CNT, the I_G/I_D ratio of these samples is considerable lower, indicating a destruction of the graphitic integrity and the subsequent formation of small graphitic fragments. A I_G/I_D ratio of around 1.0 indicates a fully oxidation of the CNT_{ox}-5 and CNT_{ox}-6 samples, while the higher intensity ratio I_G/I_D for CNT_{ox}-8 compared with the pristine CNT indicate the highly increased of the defects population.

TG-DTA

It is well known that different structural forms of carbon can exhibit different oxidation behaviour depending on the available reactive sites. For instance, disordered or amorphous carbons tend to be oxidised at around 500°C [9] because of their lower activation energies for oxidation or due to the presence of a large number of active sites. On the other hand, a well graphitized structure starts to oxidize at a relatively higher temperature, as a function of the type of CNTs.

The thermogravimetric measurements conducted on the as-received CNTs and on the oxidized samples CNT_{ox} 1-8 are presented in Figure 10.

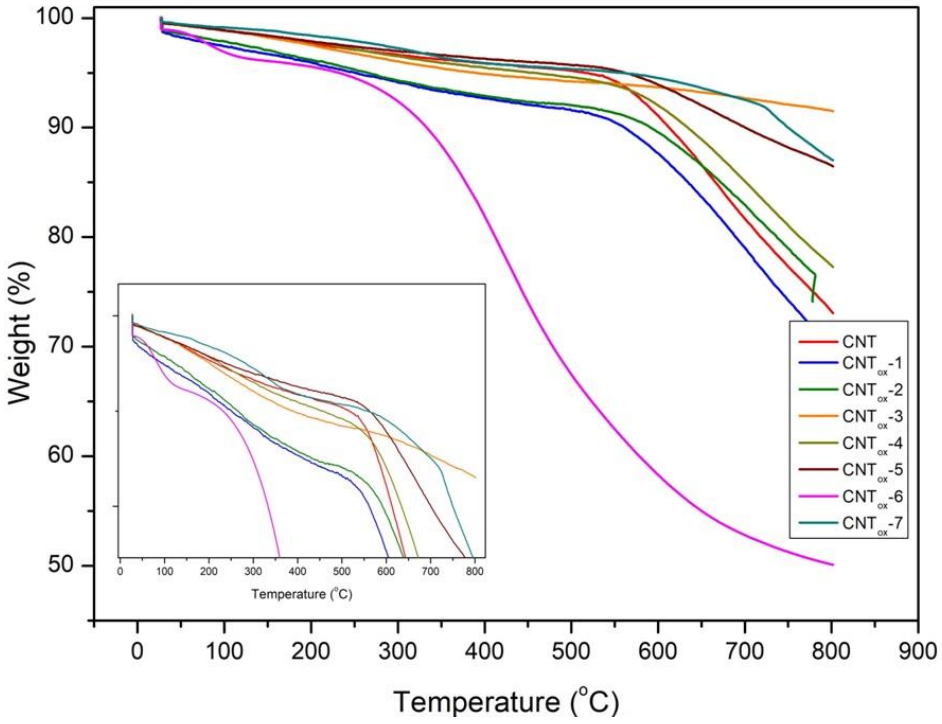

Figure 10. TGA profiles in N_2 atmosphere for CNT_{ox} 1-8 and as-received CNTs for comparison

As expected, the thermal degradation of MWCNT is a multistage process. The first step, up to a temperature of 150°C, shows a weight loss of 1-5% for the highly hydrophilic nitric acid-treated CNTs samples and for the CNT_{ox}-4 (nitric acid/sulphuric acid), which corresponds to the evaporation of the adsorbed water. The second step, from 150°C to 350°C is attributed to the decarboxylation of the carboxylic groups present on the CNTs walls. This second step appears in all the samples treated with nitric acid but do not appear in the samples treated with H_2O_2. Thermal degradation in the range of 350-500°C may be explained by the elimination of hydroxyl functionalities attached to the CNTs. This step is characteristic for the samples treated with nitric acid, and is more evident for the CNT_{ox}-6 sample, indicating the highest population of -OH groups. Finally, at a temperature higher than 500°C, the observed degradation corresponds to the thermal decomposition of the remained disordered carbon. From these results it can be concluded that the best procedure for the oxidation of multi-walled nanotubes implies nitric acid, in agree with literature reports.

Conclusions

In summary, CNT carrier was subjected to different oxidation procedures by using different oxidation agents. As characterization results showed, different kind of functional groups (i.e., carboxylic, hydroxyl and epoxy groups) were inserted on the external surface of the CNT, their nature and population highly depending on the applied oxidation procedure. Is not also excluded the formation of $-NH_2$ groups in the case of CNT oxidized with nitric acid. A too aggressive oxidation process, by using mixtures of nitric/sulphuric acids lead to a collapse of the CNT structure through its amorphization.

Perspectives

References

[1] – F.D. Schouwer, L. Claes, A. Vandekerkhove, J. Verduyckt, D. E. De Vos, Protein-rich biomass waste as a resource for future bio-refineries: state of the art, challenges and opportunities, Chem. Sus. Chem., 12 (2019) 1272-1303

[2] – W. Deng, Y. Wang, S. Zhang, K. M. Gupta, M. J. Hulsey, H. Asakura, L. Liu, Y. Han, E. M. Karp, G. T. Beckham, P. J. Dyson, J. Jiang, T. Tanaka, Y. Wang, Catalytic amino acid production from biomass derived intermediates, PNAS, 115 (2018) 5093-5098

[3] – P. Serp, M. Corrias, P. Kalck, Carbon nanotubes and nanofibers in catalysis, Appl. Catal. A: General, 253 (2003) 337-358

[4] – A. Kuznetsova, I. Popova, J.T. Yates, M.J. Bronikowski, C.B. Huffman, J. Liu, R.E. Smalley, H.H. Hwu, J.G. Chen, Oxygen-Containing Functional Groups on Single-Wall Carbon Nanotubes: NEXAFS and Vibrational Spectroscopic Studies, J. Am. Chem. Soc. , 123 (2001) 10699-10704

[5] – R. Giordano, P. Serp, P. Kalck, Y. Kihn, J. Schreiber, C. Marhic, J.L. Duvail, Preparation of Rhodium Catalysts Supported on Carbon Nanotubes by a Surface Mediated Organometallic Reaction, Eur. J. Inog. Chem., 2003, 610-617

[6] – Q.H. Yang, P.X. Hou, S. Bai, M.Z. Wang, H.M. Cheng, Adsorption and capillarity of nitrogen in aggregated multi-walled carbon nanotubes, Chem. Phys. Lett., 345 (2001) 18-24

[7] – N. Yao, V. Lordi, S.X.C. Ma, Structure and oxidation patterns of carbon nanotubes, J. Mater. Res, 13, 9 (1998) 2432-2437

[8] – B.C. Satishkumar, A. Govinndaraj, J. Mofokeng, G.N. Subbanna, C.N.R. Rao, Novel experiments with carbon nanotubes: opening, filling, closing and functionalizing nanotubes, J. Phys. B: At. Mol. Opt. Phys, 29 (1996) 4925-4934

[9] – S. Aftab, S.T. Hussain, M. Siddique, H. Nawaz, Comprehensive study of trends in the functionalization of CNTs using same oxidizing acids in different conditions, Der. Pharma. Chemica. 2 (2010), 354-365

[10] – C.P. Poole, F.J. Owens, Introduction in Nanotechnology, Wiley, 2003, Chapter 5.4: Carbon Nanotubes, 114-124

[11] – G.W. Lee, J. Kim, J. Yoon, J.S. Bae, B.C. Shin, I.S. Kim, W. Oh, M. Ree, Structural characterization of carboxylated multi-walled carbon nanotubes, Thin Solid Films, 516 (2008) 5781-5784

[12] – M.L. Toebes. J.M.P. van Heeswijk, J.H. Bitter, A. Jos van Dillen. K.P. de Jong, The influence of oxidation on the texture and the number of oxygen-containing surface groups of carbon nanofibers, Carbon, 42 (2004) 307-315

[13] – G.S. Szymanski, T. Grzybek, H. Papp, Influence of nitrogen surface functionalities on the catalytic activity of activated carbon in low temperature SCR of NO_x with NH_3, Catal., 90 (2004) 51-59

[14] – J. Zhang, H. Zou, Q. Qing, Y. Yang, Q. Li, Z. Liu, X. Guo, Z. Du, Effect of Chemical Oxidation on the Structure of Single-Walled Carbon Nanotubes, J. Phys. Chem. B, 107 (2003) 3712-3718

[15] – M.R. loos, L.A.F. Coelho, S.H. Pezzin, S.C. Amico, Effect of Carbon Nanotubes Addition on the Mechanical and Thermal Properties of Epoxy Matrices, Mater. Res., 11, 3 (2008) 347-352

[16] – V. Datsyuk, M. Kalyva, K. Papagelis, J. Pathenios, D. Tasis, A. Siokou, I. Kallitsis, C. Galiotis, Chemical oxidation of multiwalled carbon nanotubes, Carbon, 46 (2008) 833-840

[17] – S.A. Chernyak, A.S. Ivanov, K.I. Maslakov, A.V. Egorov, Z. Shen, S.S. Savilov, V.V. Lunin, Oxidation, defunctionalisation and catalyst life cycle of carbon nanotubes: a Raman spectroscopy view, Phys. Chem. Chem. Phys, 19 (2017), 2276-2285

Annex 1. Detailed oxidation procedures for the synthesis of CNT_{ox} samples.

CNT_{ox}-1: 2 g of the agglomerated MWCNTSs were dispersed in 200 mL nitric acid (65 wt%) in a 500 mL round bottom flask. In order to minimize the tubes damage, a low power sonicating bath and a relatively low acid exposure time were used. Therefore, the mixture was sonicated in a conventional ultrasonic bath for 3 h, promoting CNT disentanglement within the acid solution. In order to neutralize the strong acidity NaOH solution was added in the slurry. Then, the slurry was filtered and thoroughly washed with distilled water, until a neutral pH. Finally, the slurry was filtered using PTFE membrane filter with 0.45 μm pore sized and then dried at 80°C for 24 h.

CNT_{ox}-2: 1 g of MWCNTs were dispersed in 200 mL nitric acid (65 wt%) in a 500 mL round bottom flask. The mixture was sonicated for 3 h, promoting carbon nanotubes disentanglement within the acid solution. Next, the reaction flask equipped with reflux condenser, magnetic stirred and thermometer was mounted in the preheated oil bath and the mixture was refluxed for 1 h at 80°C and another hour at 100°C. After cooling at r.t., to the resulted slurry water was added and then filtered. The resulted solid was washed up to neutral pH and dried at 80°C for 24 h.

CNT_{ox}-3: 1 g of MWCNTs were dispersed in 200 mL of fresh nitric acid (65 wt%) in a 500 mL round bottom flask. The mixture was sonicated for 3 h in order to promote the disentanglement of CNTs within the acid solution. Next, the round bottom flask equipped with reflux condenser, magnetic stirring and thermometer was mounted in the preheated oil bath. The mixture was refluxed for 2 h at 80°C. After cooling at r.t., to the resulted slurry water was added and then filtered. The resulted solid was washed up to neutral pH and dried at 80°C for 24 h.

CNT_{ox}-4: 0.3 g of the agglomerated MWCNTs were mixed with 70 mL mixture of HNO_3 (65 wt%) and H_2SO_4 8M by mechanically stirring on a hot plate, for 15 min at 60°C and then sonicated for 2 h. Then, the slurry was filtered and thoroughly washed with distilled water, until a neutral pH. The resulted solid was dried at 80°C for 24 h.

CNT_{ox}-5: 0.3 g of the agglomerated MWCNTs were mixed with 70 mL mixture of HNO_3 (65 wt%) and H_2SO_4 3M by mechanically stirring on a hot plate for 15 min at 60°C, and then sonicated for 2 h. The solid was separated, washed with distilled water, re-immnersed in H_2O_2 (30% v/v) and the procedure was identically repeated. Then, the slurry

was thoroughly washed with distilled water, until a neutral pH and filtered. The resulted solid was dried at 80°C for 24 h.

CNT_{ox}-6: 0.3 g of the agglomerated MWCNTs were mixed with 7.5 mL mixture of HNO_3 (65 wt%) by mechanically stirring in a hot plate for 15 min at 60°C, and sonicated for 3 h. The solid was separated, washed with distilled water, re-immersed in H_2O_2 (30% v/v) and the procedure was identically repeated. The subsequent treatment with H_2O_2 was given in order to complete the oxidative process started by nitric acid, but in a gentler manner. Then, the slurry was thoroughly washed with distilled water, until a neutral pH and filtered. The resulted solid was dried at 80°C for 24 h.

CNT_{ox}-7: 0.1 g of the agglomerated CNTs were mixed with 5 mL hydrogen peroxide (30%) by mechanically stirring in a hot plate at 65°C for 72h. 2.5 mL of hydrogen peroxide was added at each 24h in order to keep a constant volume. After oxidizing the nanotubes the slurry was thoroughly washed with distilled water until a neutral pH and filtered. The resulting solid was dried at 80°C for 24 h.

CNT_{ox}-8: 0.1 g of the agglomerated CNTs were dispersed in 10 mL nitric acid (65 wt%) in a 50 mL round bottom flask. The mixture was sonicated for 3 h in a conventional ultrasonic bath Bandelin SONOREX™ SUPER with build-in heating, RK 103H, promoting CNT disentanglement within the acid solution. Then, the slurry was filtered and thoroughly washed with distilled water until a neutral pH. Recovered filter was immersed into distillated water and ultrasonated until the carbon nanotubes redispersion (2 min). The redispersed carbon nanotubes were then centrifuged for 5 min at 4000 rpm. Remained nanotubes into the liquid phase were collected by adding 100 mL dichloromethane (CH_2Cl_2) followed by filtration, whishing with additional amounts of CH_2Cl_2 and ultrasonication for 3h. The obtained solution was the subject of a slow evaporation (r.t. for 24 h). Finally, the obtained solid was completely dried at 80°C for 24 h.